8. Z. Liu, H. Lee, Y. Xiong, C. Sun, and X. Zhang, "Far-field optical hyperlens magnifying sub-diffraction-limited objects," Science **315**(5819), 1686 (2007).
9. J. Wang, Y. Xu, H. Chen, and B. Zhang, "Ultraviolet dielectric hyperlens with layered graphene and boron nitride," J. Mater. Chem. **22**(31), 15863–15868 (2012).
10. U. Leonhardt and T. Tyc, "Broadband invisibility by non-Euclidean cloaking," Science **323**(5910), 110–112 (2009).
11. T. Ergin, N. Stenger, P. Brenner, J. B. Pendry, and M. Wegener, "Three-dimensional invisibility cloak at optical wavelengths," Science **328**(5976), 337–339 (2010).
12. J. Li and J. B. Pendry, "Hiding under the carpet: a new strategy for cloaking," Phys. Rev. Lett. **101**(20), 203901 (2008).
13. U. Leonhardt, "To invisibility and beyond," Nature **471**(7338), 292–293 (2011).
14. B. Zhang, Y. Luo, X. Liu, and G. Barbastathis, "Macroscopic invisibility cloak for visible light," Phys. Rev. Lett. **106**(3), 033901 (2011).
15. X. Chen, Y. Luo, J. Zhang, K. Jiang, J. B. Pendry, and S. Zhang, "Macroscopic invisibility cloaking of visible light," Nat Commun **2**, 176 (2011).
16. J. Valentine, J. Li, T. Zentgraf, G. Bartal, and X. Zhang, "An optical cloak made of dielectrics," Nat. Mater. **8**(7), 568–571 (2009).
17. L. H. Gabrielli, J. Cardenas, C. B. Poitras, and M. Lipson, "Silicon nanostructure cloak operating at optical frequencies," Nat. Photonics **3**(8), 461–463 (2009).
18. T. Ergin, J. Fischer, and M. Wegener, "Optical phase cloaking of 700 nm light waves in the far field by a three-dimensional carpet cloak," Phys. Rev. Lett. **107**(17), 173901 (2011).
19. B. Zhang, T. Chan, and B. I. Wu, "Lateral shift makes a ground-plane cloak detectable," Phys. Rev. Lett. **104**(23), 233903 (2010).
20. D. Malacara, *Optical Shop Testing*. (2nd Edition, John Wiley Inc., Wiley-Interscience, 2007).
21. E. P. Goodwin and J. C. Wyant, *Field Guide to Interferometric Optical Testing*. (SPIE Press, 2006).
22. Y. Luo, L. J. Arauz, J. E. Castillo, J. K. Barton, and R. K. Kostuk, "Parallel optical coherence tomography system," Appl. Opt. **46**(34), 8291–8297 (2007).
23. J. M. Schmitt, "Optical coherence tomography (OCT): a review," IEEE J. Sel. Top. Quantum Electron. **5**(4), 1205–1215 (1999).

1. Introduction

Transformation optics [1, 2] has provided a new perspective with novel physical insights in light manipulation utilizing the invariance property of Maxwell's equations under coordinate transformations [3, 4]. A variety of conceptual devices can be categorized into the frame of transformation optics, such as the perfect lens [5], the hyper lens [6–9], and invisibility cloaks [1, 2, 10–18]. Compared to other light manipulation strategies, the unique superiority of transformation optics is the capability of recovering both ray trajectory and optical path length in light manipulation. However, most previous experiments focused on demonstrating the ray trajectory recovery, while the optical path length preservation property was often neglected because of the difficulty in phase measurement. It is the purpose of this paper to demonstrate recovery properties for both ray trajectory and optical path length at the same time and provide a direct and solid evidence for transformation optics strategy.

To convincingly demonstrate the recovery of both ray trajectory and optical path length, one must consider possible errors in the measurement, which scale with the size of the device itself. For devices with the size of only a few wavelengths, as in [11, 16–18] the errors are often too small to determine experimentally. For example, previous carpet cloaks designed from quasiconformal mapping [12] have been shown to be associated with lateral shift of reflected rays whose value is comparable to the hidden object [19], while this shifting phenomenon was not directly observed in most previous experiments [11, 16–18] because a subwavelength lateral shift was not easily perceivable at the nano-scale. So in this paper we instead use an easily realizable macroscopic optical transformation device, where possible errors are much larger than the wavelength and, thus, easily quantifiable.

Regarding the optical path length, or the optical path, it is possible to measure with coherent interferometry [18] but then the measurement inherently has an ambiguity of 2π; again, this may be appropriate for nano-scale devices where the error can only be a fraction of the wavelength. Since our device is macroscopic, to avoid the phase unwrapping problem we elected to use low-coherent optical interferometry.

Here, we use a simple transformation optics device of phase-preserved optical elevator that can expand the corresponding electromagnetic space and experimentally demonstrate its capability of recovering both the ray trajectory and optical path length. The optical elevator is simply made of a single piece of natural birefringent crystal with low-loss in the visible regime. The effect of the double refraction from the birefringent crystal is to "lift" upwards the apparent position of a sheet placed underneath the device, which has been observed for centuries. However, it is important to note that, fundamentally different from the other commonly observed optical illusion such as the mirage effect, the optical elevation does not alter the optical path, so that the optical elevation is phase-preserved. Despite the simplicity of this device, the relationship between the ray trajectory preservation and optical path length preservation in similar transformation has been discussed in Ref [19]. as an intermediate step for a more general transformation which led to the previously highlighted carpet cloaks [11, 12, 16–18]. Therefore, this simple device can provide a solid foundation for related transformation techniques in the development of transformation optics.

2. Design and simulation fesults

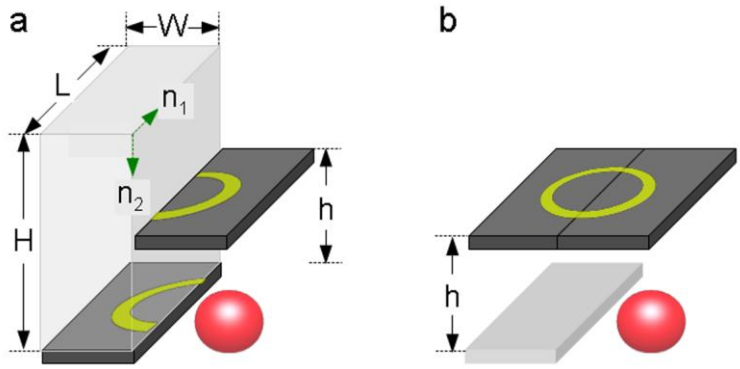

Fig. 1. (a) A cuboidal phase-preserved optical elevator is made of a single piece of natural birefringent crystal with the geometrical parameters of H = 19.8mm, L = 40mm, and W = 10mm. (b) The phase-preserved elevating design virtually lifts a sheet to a height of h = 2.2mm, enlarges the volumetric space under the sheet, and further provides the camouflage capability of exterior environment.

A schematic of the phase-preserved elevator using a single piece of a natural birefringent crystal is shown in Fig. 1. The phase-preserved elevating device has a cuboidal shape (Fig. 1(a)) to lift the apparent position of a sheet underneath (Fig. 1(b)) to an elevated height *h*. The geometrical design parameters are labeled in Fig. 1(a), and the refractive indexes of n_1 and n_2 for polarized light are ~1.66 and 1.48, respectively. The top and bottom surfaces are polished with fine optical surface quality.

Before we explain the design, we first consider a simulation of light propagation through the phase-preserved elevator, where a thin mirror sheet is placed underneath, as shown in Fig. 2(a). Using the same incident wave and background medium, Fig. 2(b) shows the simulation of light reflected by the same mirror located above the original position with an increased height of *h*. It can be seen that the phase of the light after passing through the phase-preserved elevator is identical to its counterpart in the unexpanded virtual space. As we emphasized already in the Introduction, it is this phase preservation that makes the phenomenon of lifting illusion discussed in this paper non-trivial and fundamentally different from the commonly observed lifting illusion through a high refractive index liquid (e.g. the bending of a straight pencil immersed in water).

#182521 - $15.00 USD Received 2 Jan 2013; revised 23 Jan 2013; accepted 29 Jan 2013; published 11 Mar 2013

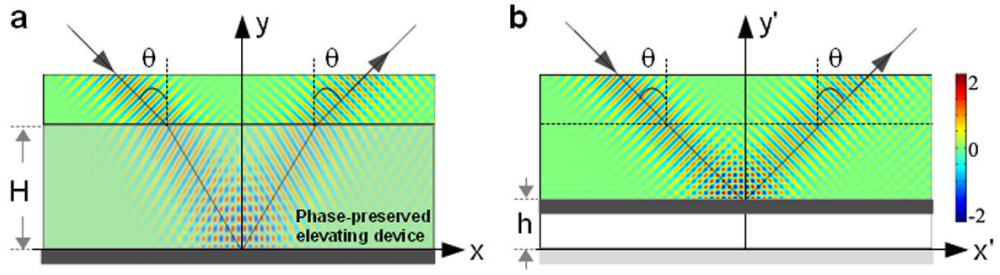

Fig. 2. Simulations of phase-preserved optical elevating effects, performed with light propagation using the software COMSOL Multiphysics. The refractive index of the surrounding media is assumed to be 1.66. Light at 561nm with the incident angle of θ passing through the phase-preserved elevator system (a) is identical to its corresponding expansive virtual space without phase-preserved elevators (b).

Now we proceed to explain the design of the phase-preserved optical elevator as well as the concrete parameters in Fig. 1. Let us first consider the following transformation from the original coordinates (x', y', z') into a new set of coordinates (x, y, z):

$$\begin{aligned} x &= x' \\ y &= \frac{H}{H-h} y' + \frac{H}{h-H} h \\ z &= z' \end{aligned} \tag{1}$$

Such a transformation expands the electromagnetic space. Therefore, through this transformation, we can obtain the following constitutive parameters for the material [1, 2] as

$$\varepsilon = \mu = \frac{J \cdot J^T}{\det(J)} = \begin{pmatrix} H-h/H & 0 & 0 \\ 0 & H/H-h & 0 \\ 0 & 0 & H-h/H \end{pmatrix} \tag{2}$$

where J is the Jacobian of the transformation between the virtual space (x', y', z') and physical space (x, y, z). Here we assume the background medium is air.

In order to make the material realizable in optical frequencies, here we consider two-dimensional (2D) geometry with vertical polarization; i.e., the magnetic field can only interact with the z-component of the permeability tensor. We then set this component equal to one, such that a nonmagnetic phase-preserved elevator can be created. Accordingly, the other components of the permittivity tensor need to be adjusted to keep the refractive index unchanged, resulting in

$$\varepsilon = \begin{pmatrix} (H-h/H)^2 & 0 \\ 0 & 1 \end{pmatrix} \tag{3}$$

This means that the permittivity can be expressed as two values in two principal directions, respectively. Please note that the above expression for permittivity is with the assumption that the background medium is air. If we choose another background medium with permittivity ε_b, the two principal permittivity components will become $(H-h/H)^2 \varepsilon_b$ and ε_b, respectively. Consequently, to fix the geometry with available natural materials, we can obtain the principal values of the permittivity as about 1.48^2 and 1.66^2, if we choose the refractive index of the background to be 1.66, H = 19.8 mm and h = 2.2 mm. This particular material can be simply realized using a single natural calcite crystal with n_1 = 1.66 and n_2 = 1.48, as shown in Fig. 1(a).

#182521 - $15.00 USD Received 2 Jan 2013; revised 23 Jan 2013; accepted 29 Jan 2013; published 11 Mar 2013

3. Experimental setup and measurements

The first step in the experimental characterization is to prove that the ray trajectory is preserved, *i.e.* to measure the position of the reflected light. We first characterize the elevating effect with various viewing angles inside a transparent liquid environment. In this measurement we adopted a transparent laser liquid (OZ IL 19513/16), from Cargille Labs, n ~1.66 measured at visible wavelength) for our position experiments. It is the same as the ideal background refractive index n = 1.66 for this experiment.

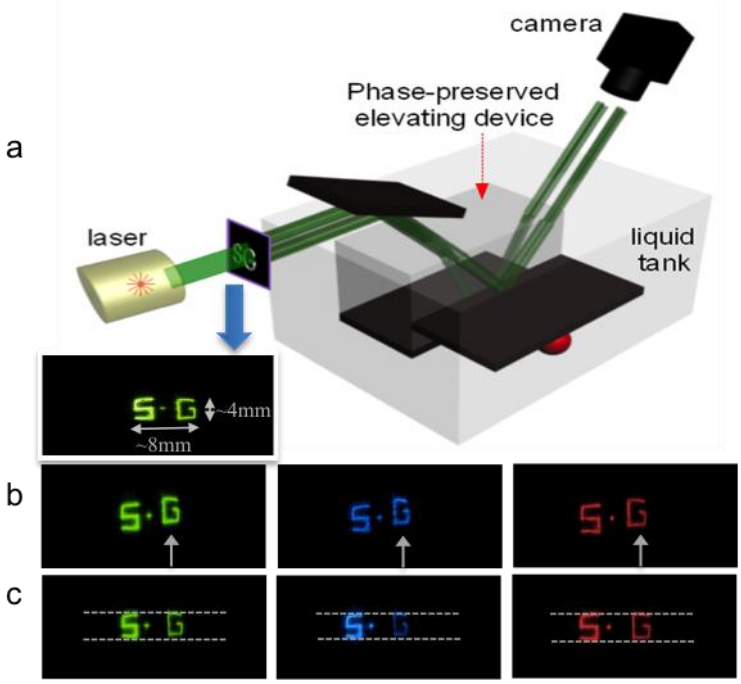

Fig. 3. Phase-preserved optical elevating using green, blue, and red laser beams. a, Schematic diagram of the experimental setup. The laser beam goes through a mask pattern "S•G", and a CCD camera is monitoring the phase-preserved elevating effect above the tank. The surrounding medium in the glass tank is first filled with a transparent liquid of refractive index ~1.66. The images captured on the CCD camera when the light through "G" is reflected by a mirror sheet placed at a height of h~2.2mm. Meanwhile, light through "S•" is reflected from the plain mirror sheet without the phase-preserved elevator (b), and with the phase-preserved elevator above the plain mirror (c).

The experimental setup for ray trajectory measurements is schematically illustrated in Fig. 3(a), where the glass tank is filled with the transparent laser liquid. To better visualize the effect of phase-preserved elevation, a mask pattern "S•G", printed on an opaque plastic plate with thickness of 1 mm using a stereolithography machine (ViperTM SLA System), is located in front of the laser-head. The pattern is placed such that the transverse magnetic (TM) polarized light that is transmitted via the symbol "S•" will go through the phase-preserved elevator with a mirror sheet underneath. Meanwhile the light going through the symbol "G" will directly be reflected by a mirror sheet's surface which is placed at the height of h ~2.2 mm with target objects underneath. A CCD (charge-coupled-device) camera is used to monitor the projected image from the opposite side of the tank. If the phase-preserved elevator can camouflage the target objects successfully, the CCD camera will image a well-patterned "S•G" as though the mirror sheet under the phase-preserved elevator were lifted up to the same height (h) of the camouflaged target objects.

#182521 - $15.00 USD Received 2 Jan 2013; revised 23 Jan 2013; accepted 29 Jan 2013; published 11 Mar 2013

This behavior was confirmed by measurements at different incident wavelengths (488nm, 561nm, 650nm) and at various angles. Figure 3(b) shows the image obtained when the light through "S•" was reflected from the plain mirror sheet surface with the incident angle θ (as shown in Fig. 2) of 25°. In the image, the symbols "S•" and "G" are located at different altitudes, being consistent with the different positions of two mirrors (as Fig. 3(a) shows). In contrast, Fig. 3(c) shows the case when "S•" is reflected from the phase-preserved elevated mirror surface; all letters in the captured CCD image are located at the same height, serving as the direct evidence of ray trajectory preservation. The lifting performance was also verified for other incident angles θ = 30°, 40 °, and 50°.

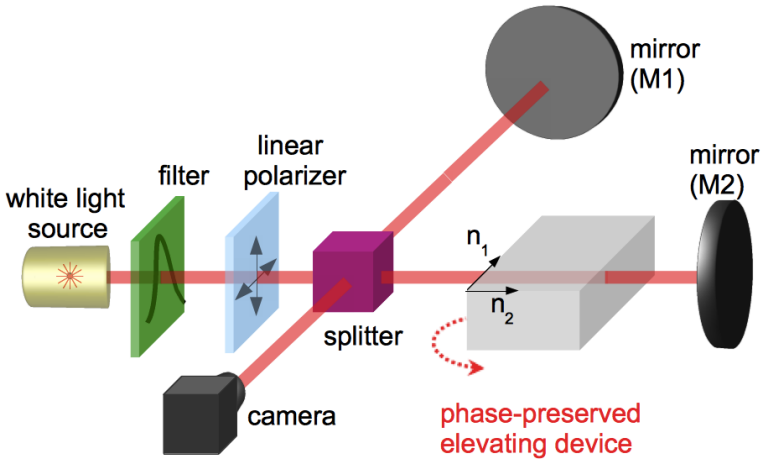

Fig. 4. Optical characterization of the phase-preserved optical elevating in free space using a low-coherence interferometer with a white light source and a linear polarizer. The elevating device is rotated with different incident angle for phase measurement.

The second step of demonstration, as the most significant evidence, is the proof of optical path length preservation, *i.e.* comparison of the optical path length through the elevator to that of unexpanded virtual space. We did this by using a white-light interferometer [20, 21], as shown in Fig. 4, to measure the optical path length preservation with high axial resolution. Ideally, we should do this in the laser liquid environment with refractive index = 1.66. However, to enhance the accuracy of phase measurement and exclude the instability from the liquid surrounding environment, we use only one piece of solid calcite (without the laser liquid) to mimic both cases with and without the elevator (in the laser liquid environment) simultaneously. We utilize Fig. 5 to justify the equivalence of the measurements without the laser liquid to those ideally with laser liquid.

Figure 5 shows the difference in optical paths of the TM wave and the transverse electric (TE) wave through a calcite crystal in a surrounding medium of arbitrary refractive index n_b. Ideally, we should locate the elevator inside the laser liquid which has refractive index 1.66. However, because the TE wave in Fig. 5 perceives the calcite crystal exactly as an isotropic medium with refractive index 1.66, we can simply rotate the polarization of incident light from TM to TE in order to obtain the optical path in the laser liquid with the same incident angle. The optical path difference (OPD) between the TE and TM waves is

$$OPD = n_1 \frac{h}{\cos\alpha} - n_b h \tan\alpha \sin\theta = h\sqrt{n_1^2 - n_b^2 \sin^2\theta} \qquad (4)$$

#182521 - $15.00 USD Received 2 Jan 2013; revised 23 Jan 2013; accepted 29 Jan 2013; published 11 Mar 2013

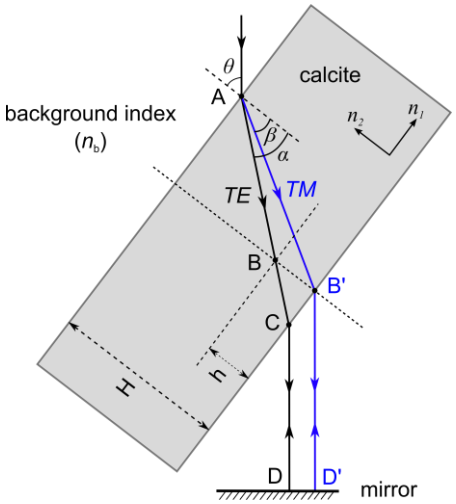

Fig. 5. Schematic of the optical paths of TM wave *(TM)* and TE wave *(TE)* in the elevator within a surrounding background medium with refractive index n_b.

The experimental arrangement of the Michelson interferometer arrangement (Fig. 4.) is illuminated with white light (Newport 300 Watt Xeon Lamp, 6258) passing through a collimator, linear polarizer, and bandpass filter. Mirror 1 defines the reference path in air, whereas Mirror 2 reflects light going through the optical elevator. The precise distance between the two paths is matched when a single (typically) interference fringe can be observed at the exit arm of the interferometer. With a filter bandwidth of 480nm (Thorlabs FGS), we calculated the coherence length of the source to be 0.27μm [22, 23], which we take as the nominal axial accuracy of the path comparison. It is less than one average vacuum wavelength, but because of the principle of white light interferometry [20, 21], no 2π ambiguity is required to be resolved.

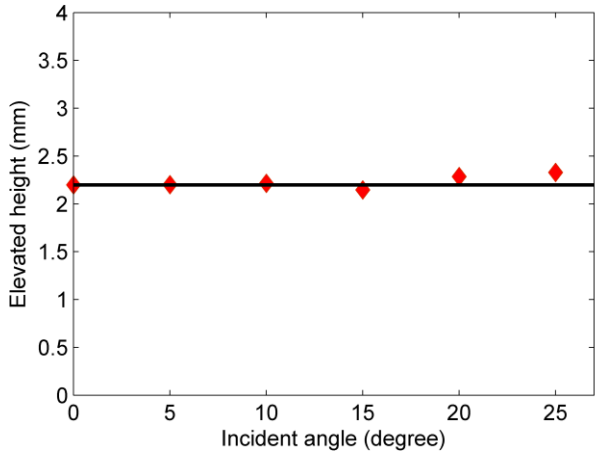

Fig. 6. Elevated height with respect to different incident angles: theoretical (black line) and experimental (red diamond) results.

Based on these elementary considerations, our experimental strategy is to carry out two measurements: one with the polarizer oriented such that only the TE wave goes through the elevator; another with only the TM wave. We then measure the corresponding optical paths by comparing the location of the reference mirror M1. We repeated this phase measurement

#182521 - $15.00 USD Received 2 Jan 2013; revised 23 Jan 2013; accepted 29 Jan 2013; published 11 Mar 2013

for different incident angles (θ) at 0°, 5°, 10°, 15°, 20° and 25°. The results are shown in Fig. 6, and show good agreement with the theoretical predictions.

4. Conclusions

In summary, we have demonstrated a phase-preserved elevator at optical frequencies using a natural birefringent crystal with low-loss and simple fabrication. In the experimental measurements, we demonstrate that both the optical phase and the position of the reflected light through the phase-preserved elevator in index-matched medium ($n_b = n_1 = 1.66$) are restored when compared to the unexpanded virtual space. To our knowledge, this is the first direct experimental characterization of the effectiveness of anisotropy in preserving both ray trajectory and optical path length in transformation optics.

Acknowledgments

We acknowledge financial support from Taiwan National Science Council (100-2218-E-002-026-MY3), National Taiwan University (101-R-7832, UN102-017), National Health Research Institutes (EX102-10220EC), the US National Institutes of Health (RO1-CA134424), the BioSystems and BioMechanics (BioSyM) Interdisciplinary Research Group of the Singapore-MIT Alliance for Research and Technology (SMART) Centre (015824-039), the Nanyang Technological University (M4080806.110), the Singapore Ministry of Education (MOE2011-T3-1-005), the National University of Singapore (R-263-000-574-133), and the Southwest University (SWU112035).

#182521 - $15.00 USD Received 2 Jan 2013; revised 23 Jan 2013; accepted 29 Jan 2013; published 11 Mar 2013